CHALMERS
UNIVERSITY OF TECHNOLOGY

Assessment of multi-fuel powered turbofans: Performance, dimensions and emissions

Downloaded from: https://research.chalmers.se, 2026-08-28 16:20 UTC

Citation for the original published paper (version of record):
Zhao, X., Grönstedt, T., KOLB, M. (2026). Assessment of multi-fuel powered turbofans: Performance, dimensions and emissions. Chinese Journal of Aeronautics, 39(9).
http://dx.doi.org/10.1016/j.cja.2026.104082

N.B. When citing this work, cite the original published paper.

research.chalmers.se offers the possibility of retrieving research publications produced at Chalmers University of Technology. It covers all kind of research output: articles, dissertations, conference papers, reports etc. since 2004. research.chalmers.se is administrated and maintained by Chalmers Library

(article starts on next page)

Chinese Journal of Aeronautics, (2026), 39(9): 104082

Chinese Society of Aeronautics and Astronautics
& Beihang University

Chinese Journal of Aeronautics

cja@buaa.edu.cn
www.sciencedirect.com

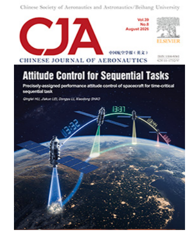

FULL LENGTH ARTICLE

Assessment of multi-fuel powered turbofans: Performance, dimensions and emissions☆

Xin ZHAO [a,*], Tomas GRÖNSTEDT [a], Moritz G. KOLB [b]

[a] *Department of Mechanics and Maritime Sciences, Chalmers University of Technology, Göteborg 41296, Sweden*
[b] *Bauhaus Luftfahrt e.V., Taufkirchen 82024, Germany*

Received 8 June 2025; revised 1 July 2025; accepted 30 October 2025
Available online 20 January 2026

KEYWORDS

Chemical equilibrium;
Emissions;
Engine performance;
Hydrogen;
Jet-A;
Multi-fuel;
Turbofan engine;
Weight estimation

Abstract This paper investigates the impact of adopting different hydrogen fuel fractions on the turbofan's design, performance, dimensions and emissions. Performance-wise, the thermal efficiency of the cycle increases by adding more hydrogen fractions into the blended fuel. By switching the fuel from 100% Jet-A to 100% H_2 at the design point, one can expect an increase up to 1% in thermal efficiency throughout a wide range of varying design parameters of specific thrust, overall pressure ratio, jet velocity ratio and pressure ratio split considering turbomachine component size correction. When fixing the design point and varying the fuel blends at critical off-design points, such as take-off, a key observation is that the combustor exit temperature could decrease as much as 70 K with an increasing hydrogen fraction. Dimension-wise, designing the turbofan with hydrogen-richer blended fuel could reduce the engine dry weight (core + fan) by up to 7%, which is mainly driven by the more powerful core with more hydrogen. The extent of benefits mentioned above is directly proportional to the hydrogen energy fraction in the blended fuel. From a first analysis of emissions using kinetics reactions with empirical residence time and primary zone fuel air ratio correction, the results show that the introduction of hydrogen has the potential of lowering NO_x emissions even with a remarkably high NO_x index. As expected, more hydrogen fractions in the fuel lower CO_2 emissions. The relatively flat CO_2 emissions index curves in the equivalence ratio range for typical turbofan operations suggest that constants can be applied for estimating the CO_2 emissions for all fuel blends. The indices are approximately 3.16, 2.38, 1.61, and 0.83 (in kg/kg fuel) for 100% Jet-A, 75%/25% Jet-A/H_2, 50%/50% Jet-A/H_2 and 25%/75% Jet-A/H_2 (in mass-based fraction) fuel blends, which are simply proportional to the Jet-A content in the fuel.

* Corresponding author.
E-mail address: xin.zhao@chalmers.se (X. ZHAO).

☆ This article is part of a special issue entitled: 'Green Propulsion' published in Chinese Journal of Aeronautics.

Peer review under responsibility of Editorial Committee of CJA.

Production and hosting by Elsevier

https://doi.org/10.1016/j.cja.2026.104082

1000-9361 © 2026 The Author(s). Published by Elsevier Ltd on behalf of Chinese Society of Aeronautics and Astronautics.
This is an open access article under the CC BY-NC-ND license (http://creativecommons.org/licenses/by-nc-nd/4.0/).

Nevertheless, the prerequisite for granting the benefit of using the multi-fuel concept is a combustion system which could deliver the same performance as the combustor of modern turbofans.

© 2026 The Author(s). Published by Elsevier Ltd on behalf of Chinese Society of Aeronautics and Astronautics. This is an open access article under the CC BY-NC-ND license (http://creativecommons.org/licenses/by-nc-nd/4.0/).

1. Introduction

Alternative jet fuels, mainly different types of Sustainable Aviation Fuel (SAF) and hydrogen, have been put under the spotlight in the aviation sector as key means to achieve net-zero emissions targets. Compared to conventional fossil-based jet fuels, SAF is thermodynamically similar but can be produced from sustainable sources and has the capability to release the same level of heat with much lower greenhouse gas emissions. Because of the similarities in terms of hydrocarbon contents, energy density, density as well as other physical and chemical properties,[1] SAF has been used for blending with conventional jet fuels as a 'drop-in' since 2008. This has largely facilitated its compatibility with current airport infrastructure and aircraft. Although pure SAF is still not allowed on commercial aircraft until today, the production and blending capacity of SAF are scaling up rather quickly[2] and the certification process of achieving 100% use is on its way.[3] Hydrogen, on the other hand, due to its very different physical and combustion properties, would require breakthroughs in onboard storage as well as new airport infrastructures for aircraft anywhere in the world.[4] As indicated by the predictions made in the ICAO report[5] on the feasibility of a Long-Term Aspirational Goal (LTAG) for international civil aviation CO_2 emission reductions, SAF has the greatest potential to reduce CO_2 emissions for aviation. Unfortunately, none of the scenarios modelled in the report could achieve net-zero CO_2 emissions by 2050 through measures within the aviation sector alone, due to the fuels' life cycle emissions.

In light of the fact that hydrogen has already been used in the production of almost all types of SAF as well as many other industrial applications, the production of hydrogen has the potential of achieving life cycle net-zero emissions.[6] The production of hydrogen may come at a high cost for development and deployment at airports, but the direct use of hydrogen as aviation fuel should be beneficial compared to SAF from a life cycle emissions perspective, as the residual carbon emissions from the different SAF manufacturing processes may not be fully neutralized. However, the direct use of hydrogen as a jet fuel is not considered as a main driver for emissions reduction by 2050 due to the low expectation of attainability and readiness of hydrogen related technologies. Nevertheless, its impact may increase in subsequent decades to further dampen the emissions from the increasing traffic volume forecast.[5] However, the prerequisite is that hydrogen relevant technologies must be commercially feasible, such as LH2 storage and transport, advanced fuel cells as well as low NO_x combustion. This poses the question: How do we de-risk hydrogen related developments and accelerate the transition to a more climate friendly fuel. The flexibility of burning blended fuel, a blend of conventional Jet-A or SAF with hydrogen, is therefore a transitional solution worth considering to kickstart the adoption of hydrogen with less risks and obstacles in a wide range of aircraft propulsion applications within the short term.

Generally, there are two options for utilizing hydrogen as a fuel for aircraft propulsion, either through electrochemical conversion in a fuel cell or by direct combustion in a gas turbine.[7] The current consensus is that fuel cell technology, due to its low specific power, is limited to short range or regional aircraft applications, or as auxiliary power units. In addition, fuel cells must compete with battery-electric powertrains, which have similar problems and may be a strong competitor to hydrogen in these markets. To fit a wider and a longer range of aircraft propulsion applications, hydrogen combustion is the choice. As concluded by Ueckerdt et al.[8], one policy recommendation from the study for the development of hydrogen is to prioritize hydrogen use for specific no-regret sectors given the short-term scarcity and long-term uncertainty of hydrogen and other electricity-based synthetic fuels, where long-distance aviation is one of the named no-regret applications as it is not only hard to abate but also impossible to be electrified.

On the roadmap of 100% hydrogen combustion, the capability of burning blended natural gas and hydrogen has been gradually enhanced towards pure hydrogen combustion.[9] As of now, research is still on going in exploring different aspects of hydrogen capable gas turbines. Examples include the studies on the combustion characteristics of blended ammonia and hydrogen,[10,11] blended natural gas and hydrogen,[12–14] blended CO and hydrogen,[15] combustion system tests with commercial gas turbines,[16,17] and further studies dealing with 100% hydrogen combustion gas turbines.[18] Similarly, for aviation, it may be interesting to investigate how different blending ratios between kerosene and hydrogen would affect the design and performance of turbofans and associated emissions. Currently, the majority of studies focusing on pure hydrogen aircraft focus on the challenges related to the aircraft design and infrastructure requirements.[19–26] Starting from a lower blend ratio, which means a lower degree of hydrogen penetration and a lower demand of on-board hydrogen storage, could be beneficial for initiating the use of hydrogen in the short-term with less risks and smaller obstacles in certification. Similar ideas can already be found in some publications with different implementations. Among them, the concept inter-stage turbine burner which equips an additional combustion chamber between the High-Pressure Turbine (HPT) and the Low-Pressure Turbine (LPT) has the potential to facilitate the use of hydrogen to a certain fraction of the total energy consumption in the second combustor without the burning of blended fuel in one chamber.[27–29]

In this paper, the multi-fuel concept refers to the combustion of blended fuel in the same combustor, which theoretically could support fuel blend ratios anywhere between 0% and 100% in terms of hydrogen fraction. Combustor compatibility enabling this capability is assumed while the results are considered at theoretical level pending combustor redesign validation. From the cycle analysis of a single shaft industrial gas turbine as conducted by Bexten et al.[30], the thermodynamic impact caused by a fuel switch from natural gas to hydrogen, for which the hydrogen content is growing progressively, is only minor to the operating point of the investigated gas turbine. However, the source of the fluid properties of different fuel combinations was not mentioned and the scope of that study focused on the variation in exhaust gas composition caused by the fuel change and exhaust gas recirculation. In addition, although the studies related to hydrogen aircraft propulsion are many, no concrete source for hydrogen and hydrogen-kerosene blended fuel properties can be found. Here in this work, chemical equilibrium was used to generate all the required thermodynamic properties in the cycle analysis. This is believed to be sufficient in order to represent the most important fluid properties and to study the impact of fuel variations on the turbofan cycle design, sizing and weight estimation of the core engine as well as major emissions trends.

In a numerical study[31] of a gas turbine combustor fueled with hydrogen and Jet-A, the authors have shown that a lower pressure loss through the combustor can be achieved by burning hydrogen rather than burning Jet-A, given the same excess air ratio. On the other hand, the combustion efficiency shows the opposite trend at a low engine speed condition in the literature due to the excess air ratio of combustion zone cannot reach stoichiometric conditions for that combustor design. Otherwise, at the other two engine speed conditions the combustion efficiency is substantially similar for both hydrogen and Jet-A across varied excess air ratios. Hence, the combustion efficiency and the pressure loss through the combustor are kept constant for all. The paper is organized as follows:

(1) Materials and methods: This section introduces the modeling tools used for simulations. It then presents the details of the blended fuel properties, including thermodynamic characteristics and combustion products. The section concludes with the design parameters and assumptions applied in the power plant cycle analysis.
(2) Results and discussion: This section first explores the isolated effects of four major design parameters on engine performance and dimensions for different fuel variations, with each parameter varied individually while the others are kept constant. Next, it discusses the impact of varying the fuel blend ratios at take-off, a critical operating condition for thermal design. Finally, it provides an initial analysis of emissions indices for typical Landing and Take-Off (LTO) cycle operations of the studied turbofan with default design values.

2. Materials and methods

2.1. Engine performance modelling and conceptual design tools

At the heart of the simulations the Chalmers in-house code for aircraft engine simulations, GESTPAN (GEneral Stationary and Transient Propulsion ANalysis),[32] is used which allows the user to perform design, off-design and transient analysis of gas turbine cycles. It has been used and validated in several projects and studies which can be found in Refs. 25,33–36. With the turbofan performance calculated, GESTPAN feeds relevant data to the weight and dimensions model WEICO (WEIght and COst estimation),[37] which is a tool that allows for the engine conceptual design and sizing. Its validation is supported by a number of projects such as VITAL[38] and NEWAC.[39] Studies using the weight estimation code can be seen for geared turbofan,[40] and for intercooled cores.[41] A computer program named Chemical Equilibrium and Applications (CEA)[42] developed by NASA was used to generate all the required thermodynamic properties. A second tool for chemical kinetics, thermodynamics, and transport processes modelling CANTERA[43] was used for cross-validation and generating combustion emissions results. The reaction models for the fuel used in CANTERA can be found in Refs. 44–46.

2.2. Thermodynamic properties and emissions characteristics of blended fuel

2.2.1. Thermodynamic properties

For conventional turbofans with kerosene-based jet fuel, the thermodynamic properties, such as the specific heat capacity at constant pressure (c_p) and the specific heat capacity ratio (γ), of the working fluid before and after combustion can be approximated with constants in a simplified cycle analysis. In addition, the gas temperature change through combustion with different Fuel to Air mass Ratios (FAR) and inlet air temperatures can be derived from a reference hypothetical composition (13.92% H and 86.08% C by weight for kerosene) and lower heating value (43200 kJ/kg) with a combustion efficiency assumption of about 0.99.[47] However, in fact these properties are a function of temperature, pressure, and gas composition. The difference between using approximated constants and using high fidelity thermodynamic process modelling tools for these properties in cycle analysis has been demonstrated in Ref. 48, in which high error values are observed at high pressures.

Within the cycle analysis performed by GESTPAN, the thermodynamic properties of the working fluid as mentioned above, as well as the specific gas constant (R) and the specific enthalpy (h), are all read from gas property look-up tables generated from equilibrium reactions using CEA. To ensure that the readings are always in the valid range, the tables are generated for different fuel/air ratios up to the stoichiometric ratio of that fuel at temperatures (up to 3000 K) and pressures (up to 200 bar, 1 bar = 10^5 Pa) in a range which is larger than required.

A sample of the thermodynamic property for 11 different fuel blends (from pure Jet-A to pure H_2 with 10% step change in H_2 mass fraction) are given in Fig. 1, where the combustion temperature rise chart (the upper chart) was created with an inlet air temperature of 950 K and pressure of 50 bar. The dots in the combustion temperature rise chart represent the FARs required for different fuel blends to achieve the same temperature rise of 650 K. This results in a combustion exit temperature of 1600 K as used in plotting the other charts of c_p and γ. Blending more hydrogen in the fuel generally shows higher values for the key thermodynamic properties with the same combustion conditions. Similar trends have already been shown for the comparison of pure hydrogen and kerosene combustion in Ref. 49.

The change of the thermodynamic properties from different fuel blend ratios can be traced back to the change in the combustion product compositions fractions, mainly the H_2O, CO and CO_2, as can be viewed in Fig. 2. These are believed to

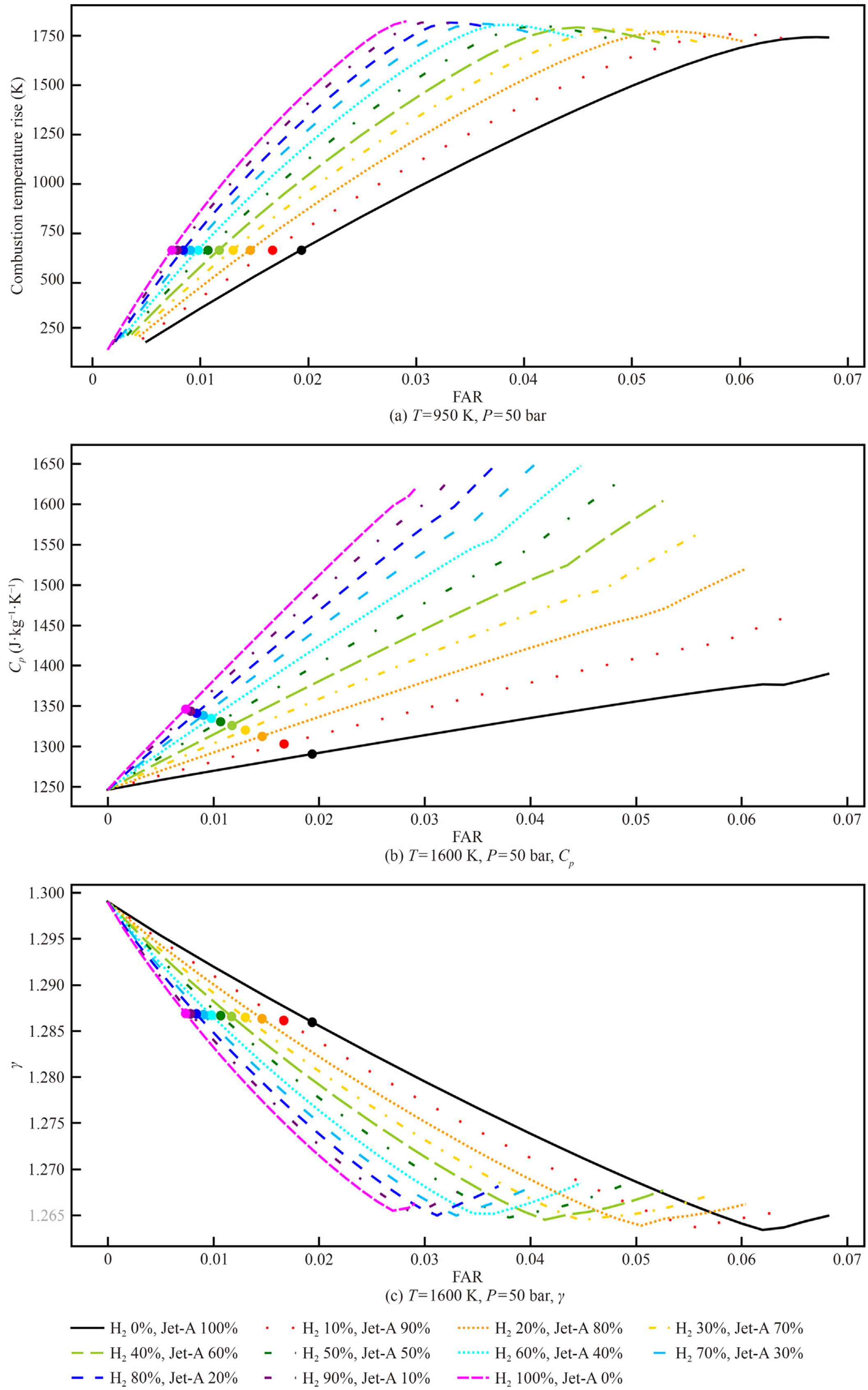

Fig. 1 Sample thermodynamic property charts for 11 different fuel blend ratios from pure Jet-A to pure H_2.

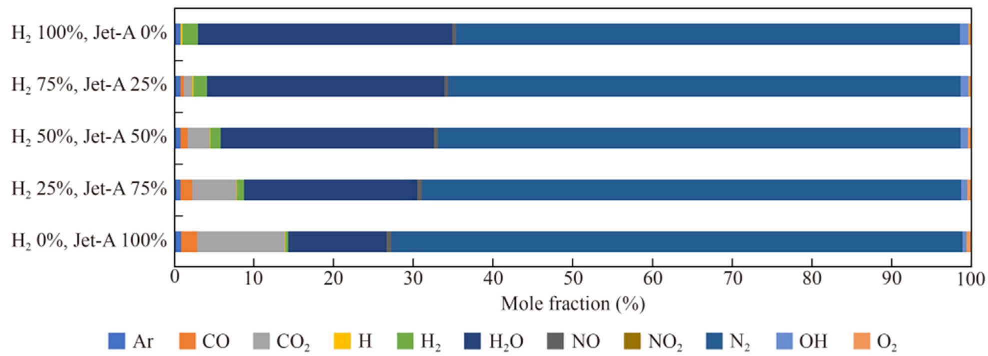

Fig. 2 Mole fractions of major combustion products for five fuel blend ratios (100% Jet-A; 75%/25% Jet-A/H_2; 50%/50% Jet-A/H_2; 25%/75% Jet-A/H_2; 100%H_2) and combustion inlet conditions 900 K/42 bar with a stoichiometric ratio.

be the key factors when the FAR is lower than stoichiometric FAR. The products from the equilibrium reactions of different fuel blend ratios present two main trends for an increasing H_2 penetration, one is the increasing fraction of H_2O, and another is the decreasing fraction of CO and CO_2. As reported by Woolley,[50] the c_p for the ideal gas state of the light isotopic water molecule is much higher than the rest of the species in the reaction products which drives the c_p higher for the fuels with increased H_2. For the FAR above stoichiometric ratio, the excessive unburnt fuel turns the curves of c_p and γ sharply.

Another observation from the charts in Fig. 1 is that the initial penetration of hydrogen has a larger effect on all the thermodynamic properties. This is simply because of the use of mass-based fractions as well as the large energy density difference between hydrogen and Jet-A. As illustrated in the charts of Fig. 3, the first 10% mass-based hydrogen penetration in the blended fuel can be translated to about 23.6% in energy fraction. Further increasing the hydrogen mass brings less and less energy-based fractions. Additionally, switching the fuel from pure Jet-A to pure hydrogen, assuming the same combustion conditions as highlighted by the dots in Fig. 1, would reduce the equivalence ratio for the combustion, reduce the total fuel mass for onboard storage by 62% and increase the total fuel volume for onboard storage by 330%. The charts in Fig. 3 are produced, assuming liquid hydrogen with a density of 70.85 kg/m^3 and a Lower Heating Value (LHV) of 120 MJ/kg.

2.2.2. Emissions characteristics

Using the combustion products from chemical equilibrium reactions, emissions indices for major emissions can be calculated. This is particularly true for CO_2; however, further corrections are required for other emissions such as NO_x, HCs, and CO. Validations given in the next section have shown that HC emissions, which are directly tied to combustion efficiency, can be well estimated from chemical equilibrium results with combustion efficiency corrections. NO_x emissions estimations from chemical equilibrium, on the other hand, showed poor agreement with high fidelity simulations and experimental results extracted from literature. This is primarily due to the fact that NO_x formation is highly time-dependent and strongly influenced by combustion parameters such as mixing quality, temperature, and pressure levels, etc.[51–54] As a result, a reaction kinetics approach following the chemical equilibrium reactions was then developed using CANTERA allowing NO_x formation to be simulated based on residence times assumed to a level matching a modern turbofan combustor, which has been used for theoretical studies on fuel blends emissions in flames.[55,56] Nevertheless, for CO formation, these simplified methods are not applicable as CO is generally considered as a transient intermediate product reflecting incomplete combustion which is highly sensitive to local conditions. In this paper, the focus is therefore on the two emissions CO_2 and NO_x which can be sufficiently well captured by chemical equilibrium and kinetics reactions with reasonable assumptions for residence times. Again, the results are considered at low fidelity theoretical level pending detailed combustor design validation.

In Fig. 4 the emissions charts of CO_2 and NO_x for five blend ratios and four combustion conditions are presented. The five blend ratios vary from pure Jet-A to pure hydrogen with a 25% mass-based fraction step of change, whilst the four combustion inlet conditions, 900 K/42 bar, 850 K/37 bar, 700 K/16 bar and 550 K/8 bar, are selected representing typical LTO cycle operating conditions take-off, climb-out, approach and idle respectively, for the studied turbofan in this paper. The relatively flat $EICO_2$ curves in the equivalence ratio range for typical turbofan operations suggest that, constants can be applied for estimating the CO_2 emissions of all fuel blends, which are approximately 3.16, 2.38, 1.61, and 0.83 (in kg/kg fuel) for 100% Jet-A, 75%/25% Jet-A/H_2, 50%/50% Jet-A/H_2 and 25%/75% Jet-A/H_2. The CO_2 from pure hydrogen combustion results from the CO_2 which is already in the air and can be neglected.

Based on the mass-based indices shown in the charts, introducing hydrogen generally increases NO_x emissions under the same combustion inlet conditions and equivalence ratio. The result curves generally match well with the study conducted by Hui et al.[56] using chemical kinetic model, though different boundary conditions have been used. Please note, the residence times for creating the NO_x charts have been assumed constant for all cases. Impacts of different residence time assumptions are discussed in the next section. The results generally agrees with a test result (inlet conditions up to 530 K and 5.4 bar covering equivalence ratio on both the lean and rich side of stoichiometry, however, actual numbers are not given only curves with trends available) from an leading industry development as reported in Ref. 57 with practical aerospace gas turbine combustor and four different configurations. For the condition with the highest inflow temperature and pressure

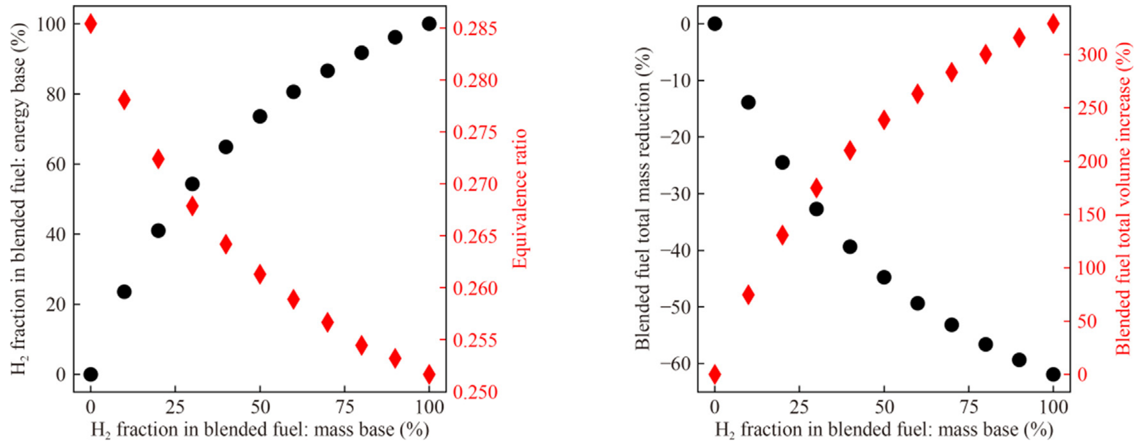

Fig. 3 Hydrogen fraction in mass base versus hydrogen fraction in energy base (black dot scale in the left), equivalence ratio for the same combustion temperature rise (red diamond scale in the left), fuel total weight (black dot scale in the right) and fuel total volume (red diamond scale in the right).

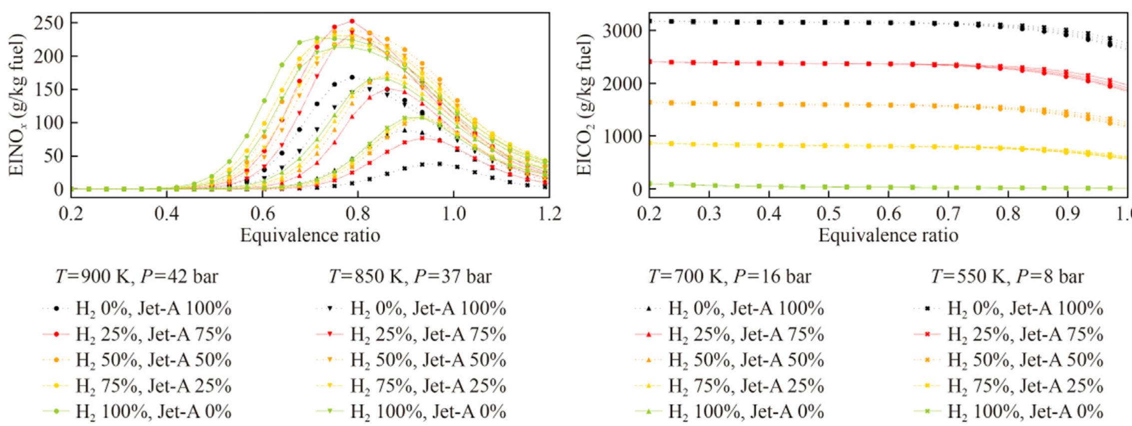

Fig. 4 Emissions indices (mass-based) for five fuel blend ratios (loosely dotted line in black: 100% Jet-A; dotted line in red: 75%/25% Jet-A/H_2; dash-dotted line in orange: 50%/50% Jet-A/H_2; dashed line in yellow: 25%/75% Jet-A/H_2; solid line with green: 100% H_2) and four representative combustion inlet conditions (●: 900 K/42 bar; ▼: 850 K/37 bar, ▲: 700 K/16 bar and ×: 550 K/8 bar).

(i.e. 900 K/42 bar), the peak NO_x emissions occur at an equivalence ratio around 0.7 which is the closest one to the value as reported in Ref. 58 for pure hydrogen combustion in a single cylinder engine. With a decreased inflow temperature and pressure, the equivalence ratio for the peak NO_x emissions increases. In addition, the equivalence ratio for peak NO_x also increases with higher Jet-A fuel composition. The reason for the higher NO_x in some cases of H_2 25%, Jet-A 75% than pure hydrogen cases is unknown. But a similar behavior was observed by Hiroyasu et al.[59], where the authors showed that NO_x index initially increases with an increase in the hydrogen addition, then drops from 10% to 30% hydrogen fraction (energy base fraction) towards higher fractions for different experimental setups. However, relatively low flow rates, 70–130 g/s, were used in these tests.

2.2.3. Validation of fuel combustion and emissions characteristics

Although there is no public data available for a direct comparison with the previously presented data, studies conducted by Kahraman et al.[31], Alabaş and Albayrak Çeper[60] and Saleem et al.[61] were used for validation. In Ref. 60, a CFD study for a mini gas turbine engine using Colorless Distributed Combustion (CDC) with varied kerosene/hydrogen blended fuels is reported. Using the equivalence ratios and input parameters of the three validation cases given in the paper, as plotted in the left chart of Fig. 5, the combustor outlet temperatures from the chemical equilibrium reaction are in good agreement with the CFD results in Ref. 60 as well as the experimental results originated from Refs. 62,63. When comparing the CO_2 emissions from varying hydrogen fractions, CO_2 emissions can be predicted with acceptable accuracy.

Unlike CDC combustion, the second validation with Ref. 31 gives larger deviations at combustor exit temperature while the gap between Jet-A and hydrogen curves is well captured, see upper left chart of Fig. 6. An explanation for this could be an inhomogeneous combustion resulting in higher temperatures compared to chemical equilibrium results. One thing worth mentioning is that, as more details are reported in the literature such as combustion efficiency and combustion zone FAR, using the combustion efficiency corrected FAR could largely improve predictions. Especially for CO_2 and HCs

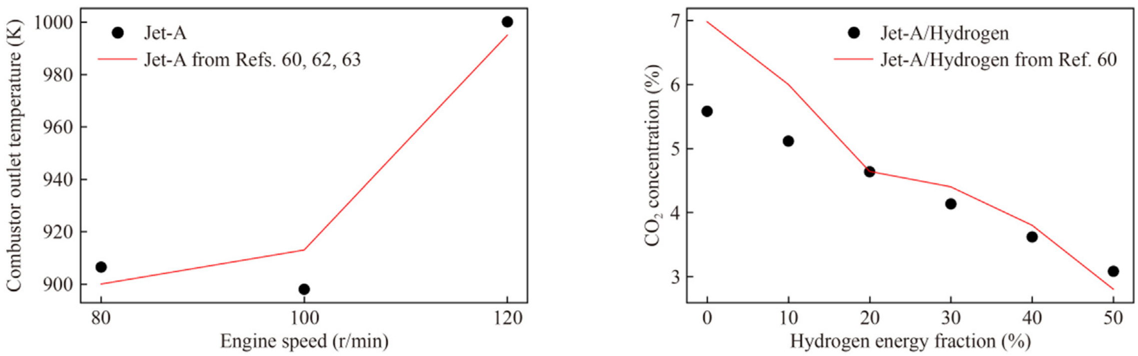

Fig. 5 Validation 1—Combustor outlet temperature and emissions comparison with Refs. 60,62,63.

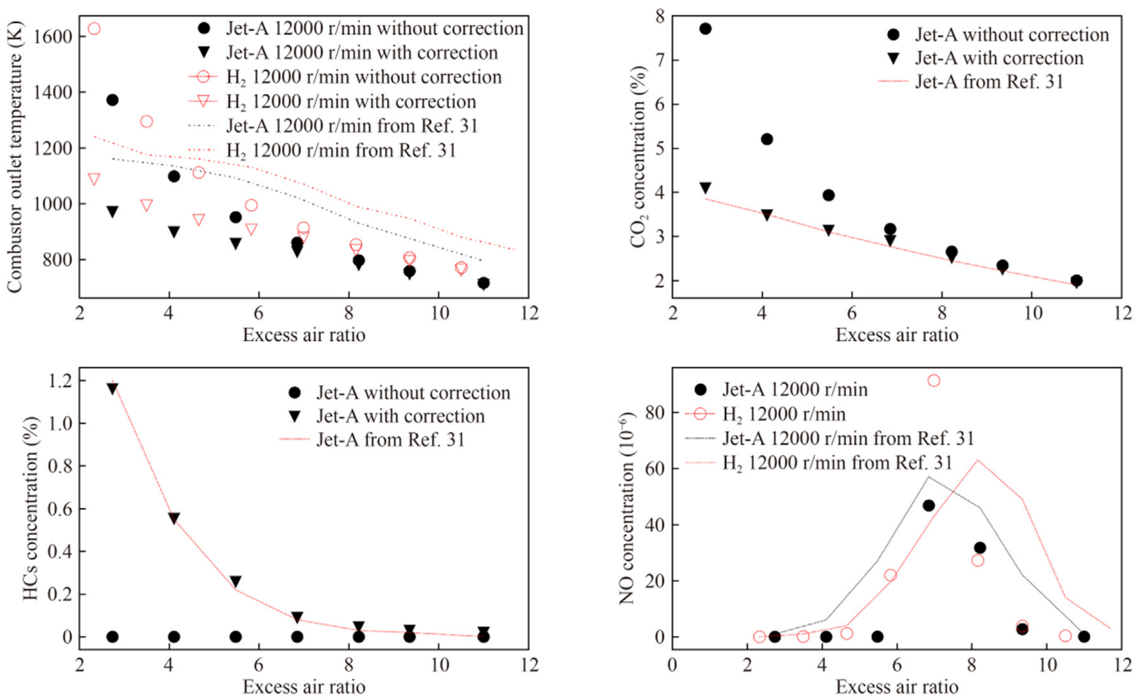

Fig. 6 Validation 2—Combustor outlet temperature and emissions comparison with Ref. 31.

emissions, the results could be matched very well with combustion efficiency corrections as can be seen from the upper right and lower left charts of Fig. 6. For NO_x emissions, since they are more sensitive to local combustion conditions, the results plotted at the lower right chart of Fig. 6 are calculated with the combustion zone FAR given in the literature. This was also demonstrated by Heywood & Mikus[54] in their study on parameters controlling nitric oxide emissions from gas turbine combustors, where they emphasized the use of primary zone FAR over overall value when predicting NO_x in low FAR regimes. This approach aligns with modern gas turbine combustor designs, which employ a small, high temperature and relatively fuel rich pilot flame in the primary zone for flame stabilization and efficient burning. This also explains that in the NO_x emissions plot given in Fig. 4, the index is remarkably low when the equivalence ratio is less than 0.4, while modern engines operating in this regime do present high NO_x emissions. A primary zone FAR multiplier, as proposed in Ref. 54, is then introduced in the LTO emissions analysis given later in the paper. This applies only for low overall FAR regimes where less than 0.3, while in the report the NO_x emissions prediction at high overall FAR regimes where around 0.6 matched well with experimental data using the overall FAR. With kinetics reaction simulation, similar levels of NO emissions are observed in this validation. This is, however, achieved through different residence times set up. For hydrogen combustion, the residence time has been set half as for the Jet-A combustion case.

The last validation presents the NO_x emissions for three blend ratios compared to the results generated by the correlation proposed by Saleem et al.[61] The correlation was a linear model with independent input variables: pressure, temperature, FAR, extent of premixing and mole fractions of blended fuel compositions including hydrogen, natural gas, ammonia and kerosene. Although the valid range for the model is limited as the foundation of the model is from published data on NO_x

emissions for various fuels under varying experimental equipment and scenarios. It is considered a strong support for the presented work. As can be seen from the comparison shown in Fig. 7, general trend of the NO_x emissions with varying fuel blends and equivalence ratios are in good agreement. One thing which has been added to the comparison is the different residence times, from 1 ms to 9 ms, set in the kinetics reaction model. With typical residence times 3–5 ms, the simulation results match the best with the correlation while the residence time has the least impact on pure hydrogen combustion.

2.3. Design parameters and assumptions in cycle analysis

A Geared Turbofan (GTF) architecture, see Fig. 8, has been selected in this study, following the performance requirements from an A320-class aircraft as shown in Fig. 9.[64] Since on-board hydrogen storage design and whole aircraft modelling is out of the scope of the paper, the turbofan operating conditions are obtained from the A320 type aircraft design without revisions to fit the hydrogen related systems and are identical to all the cases.

The key operating conditions and design ratings for the geared turbofan are listed in Table 1, with assumptions of the turbofan components key parameters given in Table 2. The assumptions were estimated based on the methods given in Ref. 65 originated from Ref. 66 with basic correlation for entry into service year, component size and Reynolds number. The aim is to identify the impact of different fuel blend ratios on the key turbofan performance parameters, such as Specific

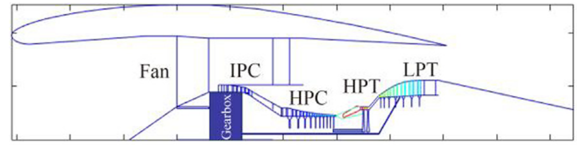

IPC—Intermediate Pressure Compressor
HPC—High Pressure Compressor
HPT—High Pressure Turbine
LPT—Low Pressure Turbine

Fig. 8 Geared turbofan layout.

Fig. 9 A320-class aircraft with year 2035 technology level assumptions.[64]

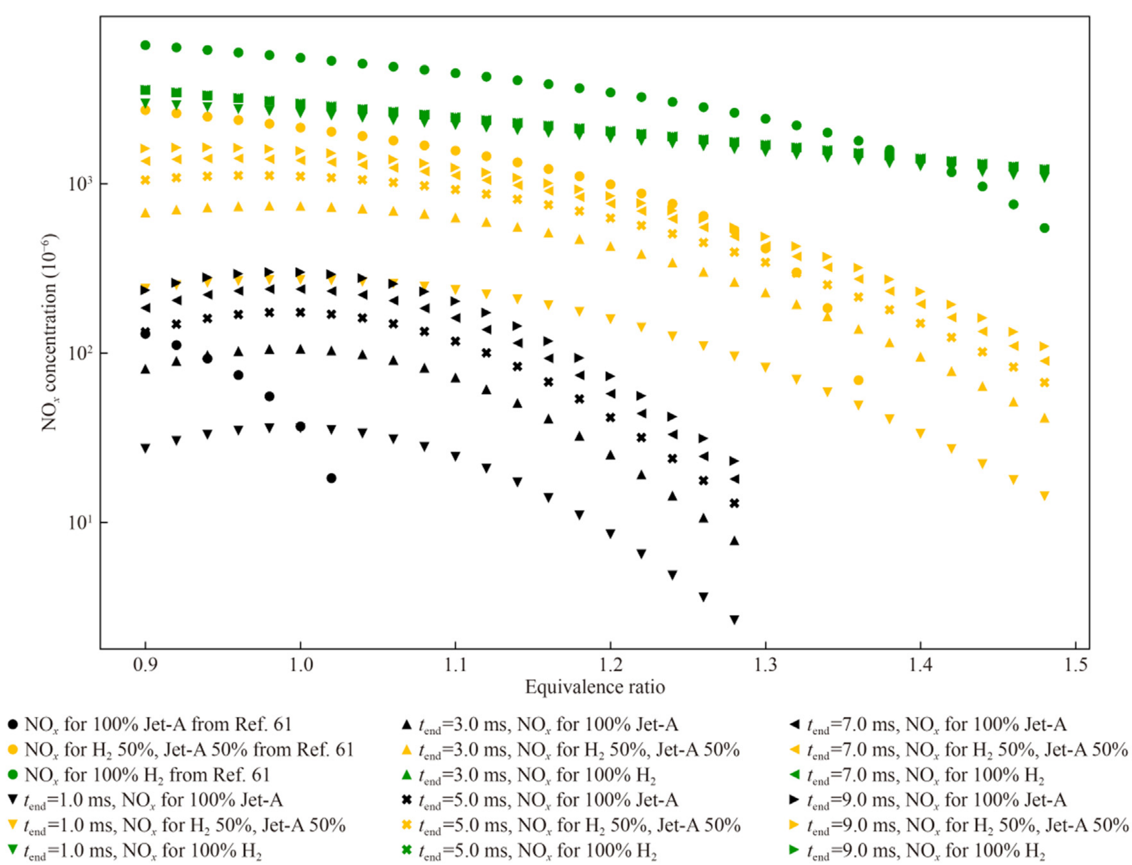

Fig. 7 Validation 3—Comparison of NO_x emissions from reaction kinetics modelling with Ref. 61.

Table 1 Turbofan operating conditions.

Operating condition	Mach number	Altitude (m)	dT_{ISA} (K)	Net thrust (kN)
Take-Off (TO)	0.2	0	+15	94.5
Top-of-Climb (TOC)	0.78	10668	+10	21.0
Cruise (CR)	0.78	10668	+0	17.0
LTO take-off	0	0	0	120.0
LTO climb-out	0	0	0	85% of LTO take-off
LTO approach	0	0	0	30% of LTO take-off
LTO idle	0	0	0	7% of LTO take-off

Notes: dT_{ISA} refers to the deviation from International Standard Atmosphere (ISA).

Table 2 Turbofan key parameters assumptions for baseline GTF establishment.

Parameter	Value
Gear box speed ratio	3.67
Fan polytropic efficiency at CR	0.94
IPC polytropic efficiency at CR	0.88
HPC polytropic efficiency at CR	0.90
HPT isentropic efficiency at CR	0.90
LPT isentropic efficiency at CR	0.94
Combustor outlet temperature at CR (K)	1588

Table 3 Design space exploration range of design parameters.

Parameter	Min	Max	Default
Overall pressure ratio OPR at CR	35	65	52
Jet velocity ratio JVR at CR	0.65	0.90	0.78
Specific thrust SFN at CR (m/s)	80	110	100
Pressure ratio split exponent PRn at CR	0.25	0.40	0.3

Fuel Consumption (SFC), thermal efficiency, propulsive efficiency and dimensions. Similar to the studies on intercooled core engine design[41,67] and hybrid turbofan performance analysis,[68,69] the following design parameters are varied to provide an overview of the impact on the key turbofan performance parameters.

(1) SFN: Specific thrust defined as engine net thrust over fan inlet mass flow.
(2) JVR: Jet velocity ratio defined as the bypass nozzle ideal jet velocity over core nozzle ideal jet velocity.
(3) OPR: Overall pressure ratio defined as the compressor exit pressure over the fan inlet pressure.
(4) PRn: Pressure ratio split exponent defined as the logarithm of the ratio of the Intermediate Pressure Compressor (IPC) exit pressure divided by the fan inlet pressure to the base of OPR.

Two sets of simulations have been conducted for the presented study. For the first set of simulations, the following parameters have been kept constant for the Cruise (CR) point: combustor outlet temperature, component polytropic efficiencies, duct, combustor, and inlet pressure losses, gearbox and shaft mechanical efficiencies, as well as HPT and LPT cooling ratios. The four design parameters are varied independently for the CR point in the range as given in Table 3, while the other three are set to the default value. Through this investigation, the impact of different fuel blend ratios on the turbofan thermal efficiency, propulsive efficiency as well as dimensions and weight are to be discussed in the later section. The thermal efficiency has been defined as the ratio of the summation of useful energy at each nozzle exit divided by the fuel heat input. When calculating the fuel heat input, 43.2 MJ/kg for Jet-A and 120 MJ/kg for hydrogen, were assumed for the lower heating values of the fuels. For blended fuels, the lower heating values have been simply approximated with the average of fractions.

The second set of simulations has been carried out with the amount of the cooling flow calculated for the HPT turbine blade temperature limit of 1240 K at Take-Off (TO). In this setup, all the parameters mentioned above in the first set of simulations have been kept constant. The only varied parameter is the fuel blend ratio for TO, while the cooling flow is varied as it is computed based on the TO operating condition. This setup is aimed at investigating the impact of changing the fuel on the off-design performance as well as turbine cooling need. In both sets of simulations, TOC has been selected to size the turbofan. The cooling model is based on the model described in Refs. 70,71, for which Thermal Barrier Coatings (TBCs), convection cooling, film cooling, and internal cooling mechanisms are considered. To estimate the required cooling flow rates, several key parameters have been identified that may be influenced by the combustion of hydrogen instead of conventional jet fuel. These include the TBC Biot number, combustion pattern factor, cooling flow factor, and film cooling effectiveness. Due to the increased water vapor content in hydrogen combustion products, there may be implications for TBC material performance. However, in the absence of publicly available data on TBC behavior under such conditions, it has been assumed that the same performance remains applicable. The combustion pattern factor is expected to be higher for hydrogen combustion, potentially resulting in increased peak temperatures at the turbine blade inlet. However, this effect is dependent on combustor design, such as the distance between the combustor exit and turbine inlet, and not recognized as a very significant parameter according to the sensitivity study reported in Ref. 70. The cooling flow factor, defined in relation to the ratio of specific heats between the combustion gas and coolant flow, is anticipated to increase under hydrogen combustion due to the higher specific heat of the combustion gases. Additionally, film cooling effectiveness may be adversely affected. The study by Jeong et al.[72] reported a reduction in film cooling effectiveness of approximately 2.5%–3% as the hydrogen blending ratio increases from 0 to 100%. To evaluate the influence of these parameters on cycle efficiency, the sensitivity analysis conducted by Ref. 70 is referenced. Based on this work, a reduction in film cooling effectiveness due to hydrogen combustion may result in an estimated 0.15% decrease in cycle efficiency. However, this loss may be partially offset by an increase in the internal cooling factor. While uncertainties remain, particularly pending combustor design validation, the associated errors are considered negligible for the scope of the present study, for the purposes of preliminary system-level cycle analysis.

3. Results and discussion

3.1. Performance and dimensions

3.1.1. Varying SFN independently

To ensure the clarity of the figures in this section, within the first set of simulations, only the results of five mass-based fuel blend ratios are shown, which are 100% Jet-A, 75%/25% Jet-A/H_2, 50%/50% Jet-A/H_2, 25%/75% Jet-A/H_2, and 100% H_2. Fig. 10 shows the results varying the first design parameter SFN at CR while OPR, JVR and PRn are fixed at 52, 0.78 and 0.3 respectively. The most pronounced results are the increasing Fan Pressure Ratio (FPR) and the decreasing propulsive efficiency with an increasing SFN, which was observed in previous turbofan studies.[41,67,68] As expected, the change of fuel blend ratio has no effect on the impact of varying SFN, so the curves of the above-mentioned parameters coincide. On the other hand, although the trends are identical, changing the fuel blend ratios does have an impact on the flow split between the core and the bypass, hence the Bypass Ratio (BPR). More hydrogen in the blended fuel results in a more powerful core hence a larger BPR, which is mainly contributed by the higher c_p of the gas leaving the combustor.

From the perspective of exergy analysis, having more air exposed to the combustion process increases exergy destruction as illustrated by Aygun[73] and a smaller core potentially experiences less exergy destruction in the core components[35] given the same SFN, OPR and combustor exit temperature. This can be a plausible reason for a higher thermal efficiency by burning more hydrogen. The improvement in thermal efficiency obtained throughout the range explored is substantially constant at about 1.25%. One thing that must be noted is that the smaller core could offset part of the thermal benefit. Taking into account the component size correction as introduced by Rolt et al.[74], the thermal efficiency improvement will be reduced to around 1%.

In addition to the improvement of thermal efficiency, less core air also results in less heavy turbofan core components when burning the fuel with increased hydrogen fractions. Remarkably consistent improvements have been observed for both the thermal efficiency and core components weight across the explored range of design parameters, which are generally proportional to the hydrogen fractions in the fuel. Nevertheless, the stage count change in the High Pressure Compressor (HPC) gets delayed with more hydrogen in the blended fuel when the SFN increases. Under the same conceptual design rules, this is the result of a lower HPC installation position from a decreased fan size and a pre-fixed inter-compressor duct radius ratio and compressor tip speed.

3.1.2. Varying JVR independently

Subsequently, the results of varying the JVR at CR are given in Fig. 11, with OPR, SFN and PRn fixed at 52, 100 m/s and 0.3 respectively. The varying JVR at CR was achieved from varying the FPR at CR. As suggested in Ref. 75, the optimal JVR is reached when the value approaches the product of the isentropic efficiencies of the fan, LPT and the bypass duct. From the assumed component efficiencies, this product is around 0.86, which marks the near optimal SFC for all the assessed fuel blend ratios, as can be seen in Fig. 11. Similar to what has been observed from the cases with varying SFN, no major difference could be found in the trends of varying JVR for the presented performance and dimension parameters. More specifically, the change of fuel blends and associated combustion products does not have a significant impact on the transfer efficiency determined by the fan, LPT and shaft efficiencies and bypass duct and jet pipe losses.

Looking closer at the propulsive efficiency curves, slightly higher values can be observed for fuel blends with higher hydrogen fractions in the low JVR range of 0.65–0.75 while an opposite behavior can be found in the JVR range of 0.8–0.9. This may be explained by the different fuel flows added to the core jet, which slightly changes the specific thrust as this is normally defined with the fan inlet air mass. At low JVR, the higher fuel mass, when operating with more Jet-A fractions, increases the core jet energy and hence lowers the propulsive efficiency calculated for the fixed flight speed and net thrust requirement. With increasing JVR, the impact of the core jet on the propulsive efficiency deteriorates as the bypass jet velocity increases while the hot jet velocity decreases. Combining the higher BPR while burning the fuel with more hydrogen leads to a decelerated increase in propulsive efficiency. For the same reason, the LPT stage count increase due to the high JVR. The associated FPR increase comes earlier for the cases with more hydrogen in the fuel. Overall, the benefits observed in thermal efficiencies and core component weights remain at the same levels for higher hydrogen fraction blended fuels.

3.1.3. Varying OPR independently

For the investigation of varying OPR, the JVR, SFN and PRn are fixed at 0.78, 100 m/s and 0.3 respectively. From this variation, the most remarkable result in the performance parameters shown in Fig. 12 is that the optimal OPR shifts towards higher values for the cases with more H_2 in the fuel. This can be explained, again, by the smaller core with more hydrogen fraction mixed into the fuel. As turbine cooling air flow losses increase with higher OPR, the smaller core with less exergy destruction caused by turbine cooling could delay the offset of the thermal efficiency benefit by increasing the OPR. The higher optimum OPR, however, could drive the last compressor blade to be even shorter and hence increases the efficiency penalty for the HPC and even the High Pressure Turbine (HPT).

The stage count of the compressors increases as the OPR increases. Since the pressure ratio split exponent PRn is fixed at 0.3, this means that the HPC must compensate the OPR rise. Hence, a more frequent stage count change in the HPC is expected and can be observed from the step change in

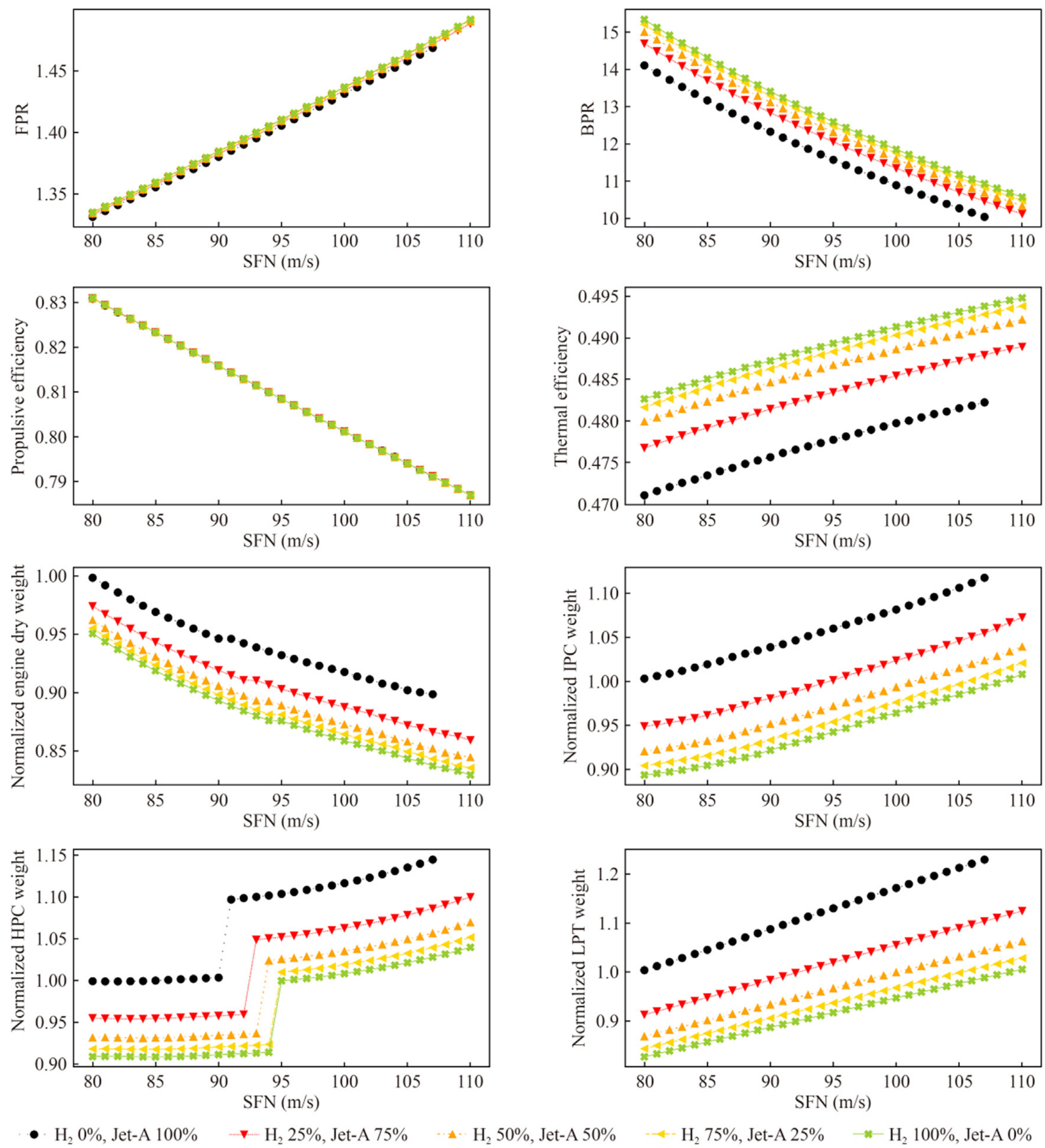

Fig. 10 Performance results at CR (top) and sizing and weight results (bottom) with varying specific thrust.

HPC weight as shown in the plot. Interestingly, for the designs with hydrogen-richer fuel the IPC stage count change occurs earlier than the ones burning more Jet-A fraction fuel, but the HPC stage count change is delayed. Whilst the HPC tip speed is set, the IPC tip speed is determined by the fan tip speed, the fixed gear ratio and its installation location. For the power plant designed with more hydrogen, the smaller core has a direct impact on the IPC stage loading leading to an earlier demand for an additional stage to fulfill an increased pressure ratio requirement.

3.1.4. Varying PRn independently

The final design parameter to be varied is the PRn. Typically, the PRn has the least impact on the performance of a simple cycle. In general, increasing the PRn for a given OPR leads to an increased pressure ratio load on the IPC and therefore reduces thermal efficiency and increases the SFC, as can be seen from Fig. 13. This is expected as the IPC works less efficiently than the HPC and the compressor exit temperature rises with poorer efficiency. Meanwhile, the core components stage counts change is almost at the same pace for all cases.

3.1.5. Varying off-design point fuel blend ratios

For the second investigation, the design parameters at the design point have been kept the same, while the fuel blend ratio in one of the off-design points, the TO point, varies from 0 to 100%. Different lines with markers in Fig. 14 represent different cases with fuel blend ratio at design point from 100%/0 Jet-A/H_2 to 0/100% Jet-A/H_2, where the horizontal axis gives the varying fuel blend ratios at TO. Comparing

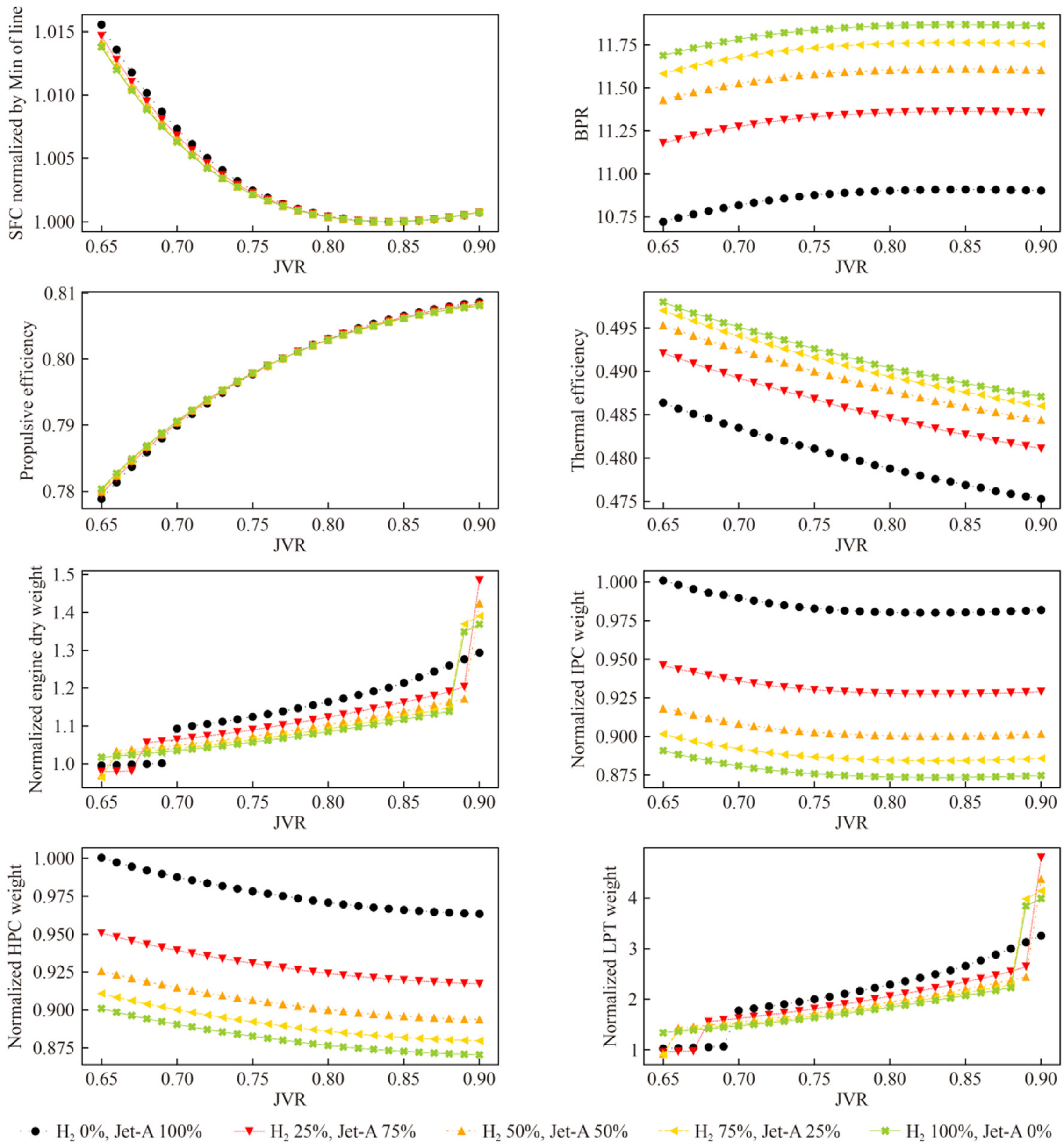

Fig. 11 Performance results at CR (top) and sizing and weight results (bottom) with varying jet velocity ratio.

the different curves, one can notice that, for a given combustor outlet temperature at design point and a given fuel blend ratio at TO, the combustor outlet temperature at TO increases with higher H_2 fractions compared to the blend in the design point. This is one of the main drawbacks of the smaller core as a result of increased hydrogen fractions in the fuel for design.

Whilst looking at a single curve, all the curves generally present the same trend. That is, for a given combustor outlet temperature at design point and a given fuel blend ratio at design point, the combustor outlet temperature at the off-design point in TO decreases with higher hydrogen fractions in the fuel which is used at TO. The differences between the combustor outlet temperatures at varying fuel blend ratios in TO could reach temperature differences up to 70 K. Similar trends have been observed in Refs. 76,77. This can be explained, again, by the higher c_p of the gas after burning more hydrogen content, which brings down the requirement of temperature drop through the turbines for a similar power requirement. By subtracting the turbine exit temperature T_5 from turbine inlet temperature T_4, one can see that the temperature drop for the expansion process reduces by about 37 K from burning 100% Jet-A to burning 100% hydrogen at TO. Looking at the turbine cooling demand, as the compressor outlet temperature does not change much for all cases, the best choice is to design the engine with 100% Jet-A and operate with 100% hydrogen at TO for minimizing the cooling flow need. Nevertheless, repeating the same test for cruise condition gives relatively low variations in combustor outlet temperature with varying fuel blend ratio. This means that this effect is more pronounced in operating conditions with high FARs.

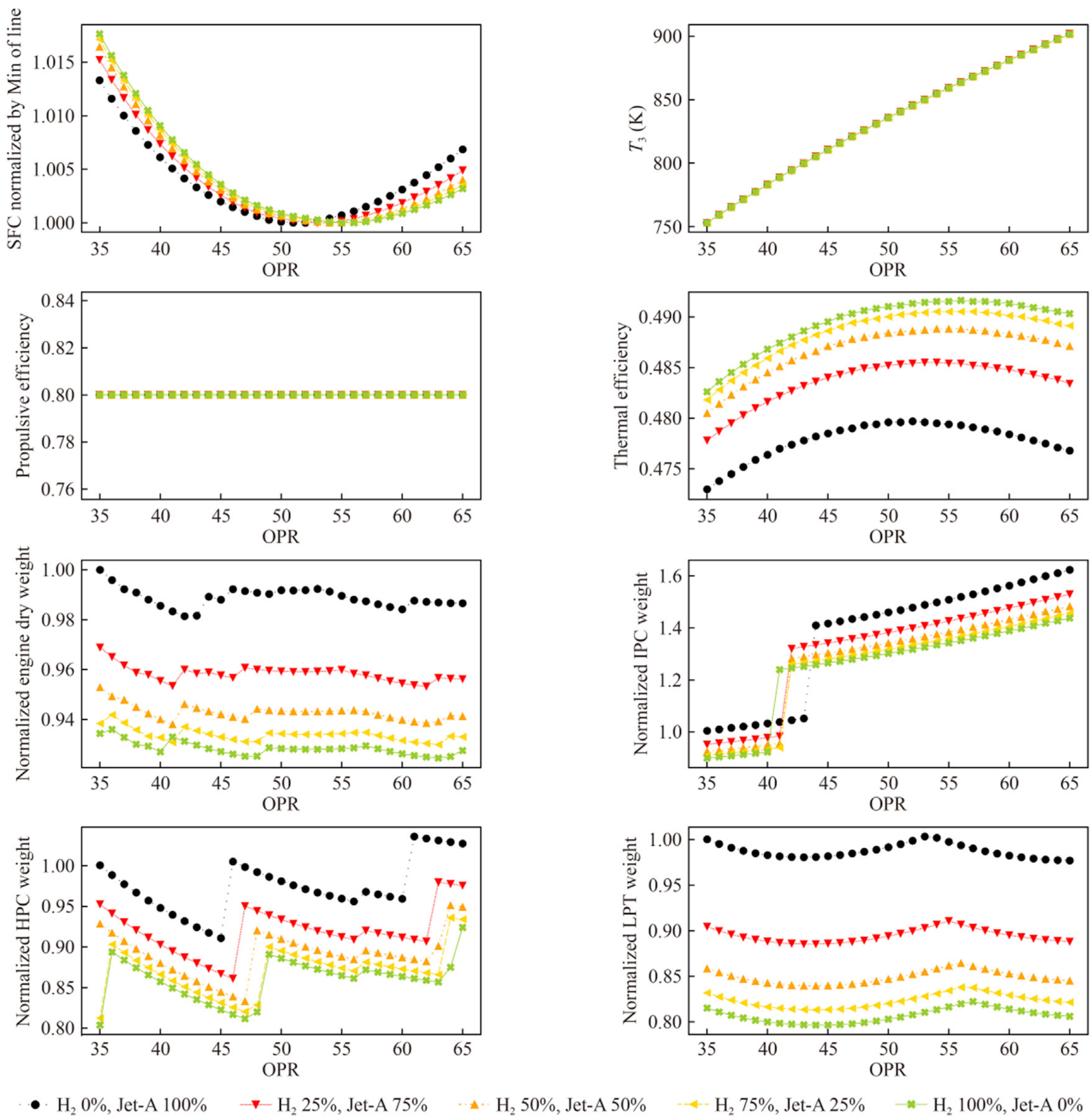

Fig. 12 Performance results at CR (top) and sizing and weight results (bottom) with varying overall pressure ratio.

3.2. Emissions for LTO cycle

Throughout the ranges of the selected parameters in the above-mentioned results, the turbofan powered with more hydrogen offers quite stable benefits on performance and weight over the 100% Jet-A powered variant, while the benefits are in general proportional to the hydrogen energy shares in the fuel. More interestingly, the combustor operating temperature's variation from varying the off-design point fuel blends could deliver additional benefits on emissions, compensating for part of the fact that burning hydrogen would result in higher $EINO_x$ as shown in Fig. 4. A detailed comparison of the LTO cycle emissions indices for the turbofans designed with the default values as given in Tables 1–3 is presented in Table 4. For each of the turbofan designs, two fuel blends are used in off-design points, one is 100% Jet-A and another is 100% hydrogen. For the NO_x estimation, kinetics reaction method used to establish the emissions characteristics as given in Fig. 4 was used for the assessment, with primary zone FAR multiplier, as proposed by Heywood and Mikus,[54] applied. Through matching typical modern gas turbine $EINO_x$ as published in report[78] for Jet-A variants, the values of the multipliers are set to 1.8,1.8, 2.4, 3.5 for the LTO take-off, climb, approach and idle respectively.

As can be seen from Table 4, the $EINO_x$ shows that the index could be 1.3–2.5 times higher for the turbofans running at 100% hydrogen, in comparison with burning Jet-A for different LTO cycle operating points. The hotter the working condition, the larger the difference. But when considering the 2.8 times higher FAR with burning Jet-A, the NO_x mass emitted is lowered. While the uncertainty of the NO_x emissions reduction is high, the CO_2 emissions reduction is nearly certain that can be reduced by 99%, as the remaining 1% of CO_2 is already present in the atmosphere.

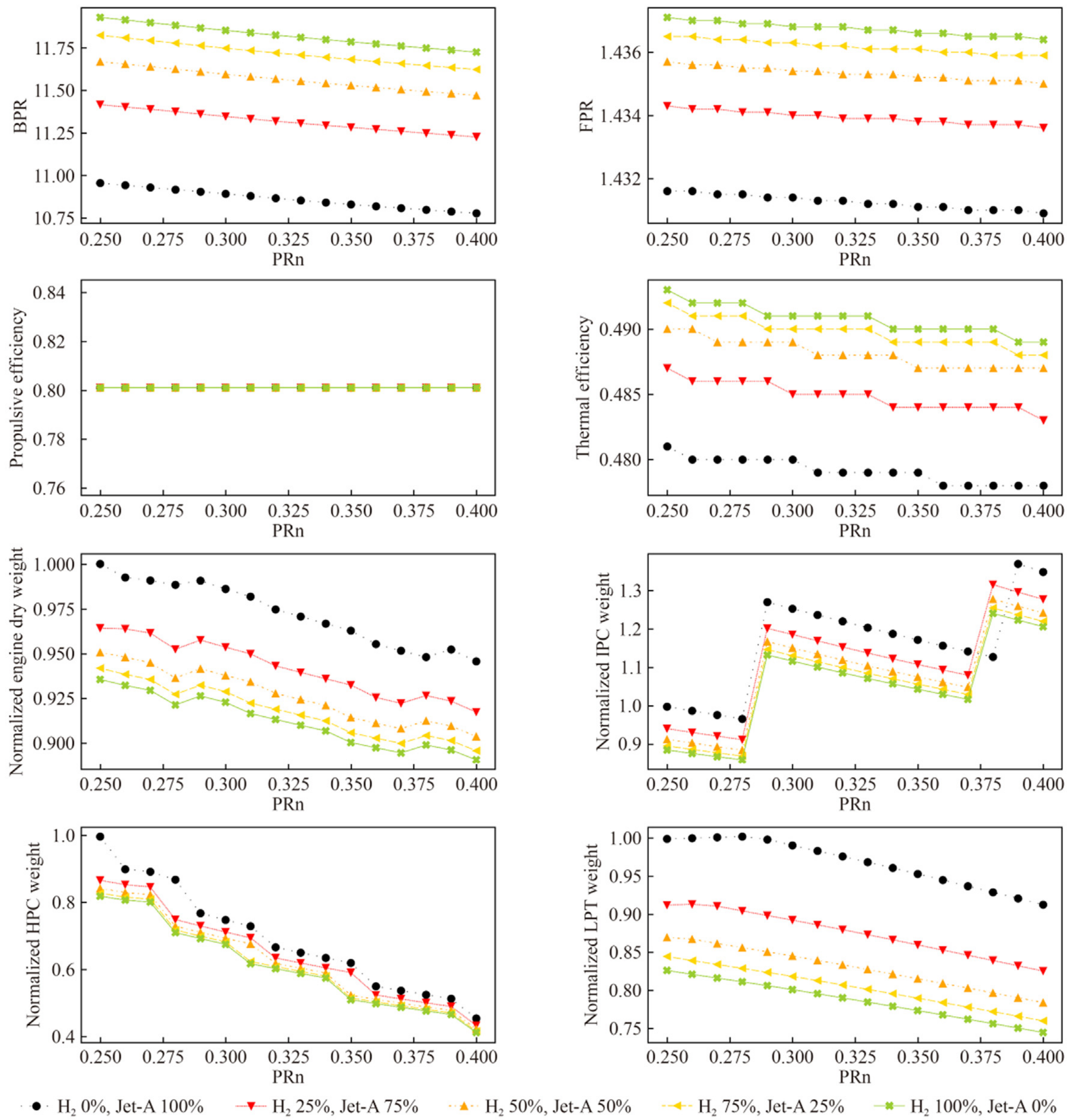

Fig. 13 Performance results at CR (top) and sizing and weight results (bottom) with varying pressure ratio split.

4. Uncertainties, limitations and future outlook

Since the presented study focuses on the assessment of the multi-fuel powerplant, limitations exist mainly on the scope that no aircraft level trade-offs have been included and discussed. As can be seen from Fig. 3, the fuel required volume increases excessively along with the hydrogen fraction increase and would have a large impact on aircraft weight, energy consumption, range and payload. A wide range of studies regarding hydrogen aircraft design generally concludes large penalties due to the use of hydrogen and associated weight and volume of the tanks compared to conventional aircraft. This includes, to name a few, energy penalties of 10%–40%,[79] increased energy consumption between 20% and 70% depending on the storage technology,[25] increased direct operation cost of 95%,[80] increased operating empty mass of 11%–27% and increased specific energy consumption of 3.3%–13% for short-and-medium range class design,[81] increased block-energy consumption of 6.5%–7.5%,[82] increased aircraft mass by 13% for 19 passenger commuter aircraft,[20] and increased energy consumption of 9%,[83] etc. Nevertheless, most studies do not consider the top-level design requirements for the propulsion system would be significantly affected, as one may sacrifice capacity or range for achieving similar aircraft maximum take-off weight. More importantly, the presented concept shows a way to ease these penalties – through the introduction of hydrogen as a "drop-in" fuel – in the short term to kick start the use of hydrogen in aviation in practice.

Large uncertainties lay on the estimation of the NO_x emissions which largely relies on the combustor development for Jet-A and hydrogen blended combustion. On the positive side, the introduction of hydrogen can improve the flame stability as reported by Hiroyasu et al.[59], appeared mainly in the primary

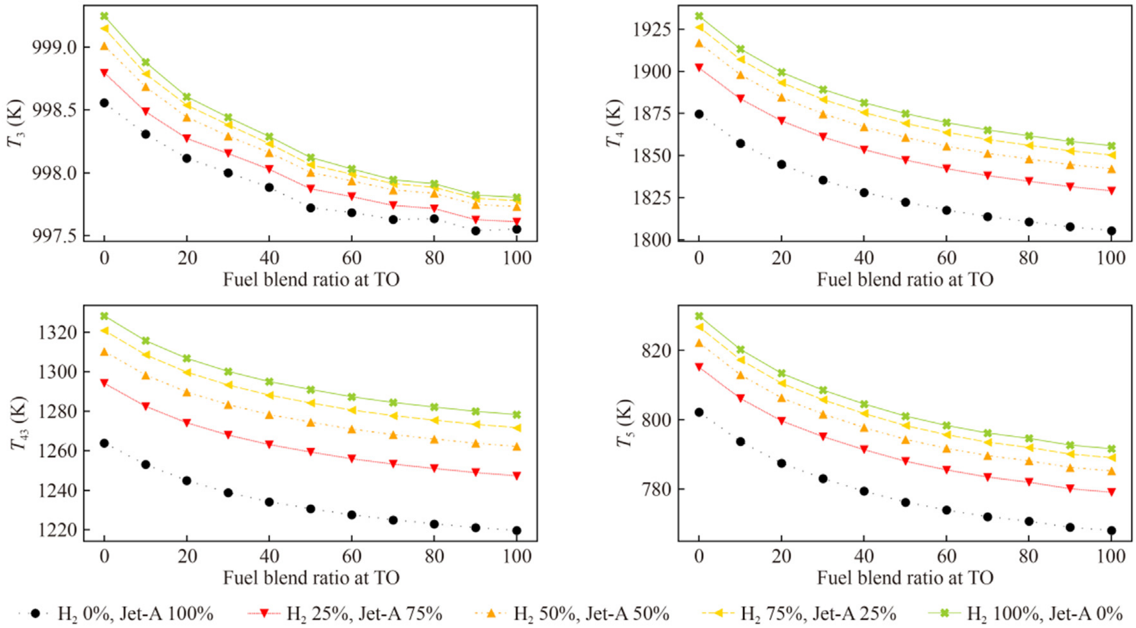

Fig. 14 Fuel blend ratio versus performance parameters at take-off off-design point.

combustion zone, where lean combustion can be easily realized. Studies of a micro-turbine jet engine incorporating hydrogen micromix diffusion combustion technology used to achieve homogeneous mixture preparation and low emissions demonstrate that NO_x emissions can be below 2×10^{-5} experimentally.[52] Low emission combustors using Lean Direct Injection (LDI) developed by NASA[84] have demonstrated that the practical designs of hydrogen injectors for LDI could result in comparable NO_x emissions levels to the Jet-A LDI combustor concepts. Except for the studies regarding pure fuels, a multi-fuel concept study within EU project HOPE conducted by Dave et al.[85] has investigated the macroscopic properties of kerosene-H_2 blended flames, which has demonstrated the capability of testing a full range of blend ratios.

On the other hand, challenges however in presence also because of the advantages of high temperature and high flame speed of burning hydrogen. As have been shown in Fig. 4 and the study conducted by Hui et al.[56], with equivalence ratio higher than 0.5, the NO_x emissions from adding hydrogen would be increased rapidly. But as mentioned above, this drawback could be mitigated by the use of lean burn technology. For the higher risk of flashback which can be detrimental to the engine, studies of using Axial Air Injection (AAI) have demonstrated the capability of flashback resistance improvement.[86–88] Specific to the multi-fuel concept, a study[89] within EU project HOPE has also deployed AAI and found that the most suitable position for kerosene injection is on the axis of the burner surrounded by hydrogen injection and air flow.

An interesting insight for future outlook would be replacing Jet-A with SAF in the fuel blends, as mentioned in the introduction, SAF itself has been certified as one of the most promising alternative fuels for reduction emissions. Different SAFs could present different fuel properties and combustion characteristics. An experimental study[90] in different SAFs has demonstrated that, while Jet-A1 performs overall better than most SAFs in fuel consumption, emissions results with different SAFs and fuel blends are a mix. For emitted particle numbers, SAFs generally provides better performance with up to 100% reduction, but in terms of NO_x and CO the performance is similar or slightly worse. Another minor factor is the fuel purity, while jet fuels, even SAFs, could contain sulfur content and emit SO_2; hydrogen on the other hand, could contain a very low level of methane $< 1\%$ from production. For the focus in the paper, these factors were, however, not considered as the very small amount of those elements contributes little to the combustion and emissions characteristics and would not change the conclusion.

5. Conclusions

In this paper, to ease the adoption of hydrogen with less risks and obstacles in aircraft propulsion applications within the short-term, a power plant concept, which can use hydrogen and Jet-A blended fuel, has been investigated. Through the conceptual design and first analysis of emissions for a wide range of multi-fuel geared turbofan designs with the fuel characteristics established by chemical equilibrium reaction models, the main results are concluded as follows:

(1) The thermal efficiency of the cycle increases with adding more hydrogen into the blended fuel, which is generally proportional to the energy fraction of the hydrogen in the fuel. The first 25% of hydrogen mass fraction in the blended fuel, which is about 48% energy fraction of the fuel, delivers half of the benefit which can be obtained from switching the fuel from 100% Jet-A to 100% hydrogen. For adopting 100% hydrogen, one can expect a maximum increase of 1.25% in thermal efficiency while keeping the same propulsion efficiency. Taking account of component efficiency drop due to a smaller core for the hydrogen turbofan, the increase will be reduced to around 1%.

Table 4 LTO cycle combustion parameters and emissions indices for selected turbofan designs.

Operating condition		FR_d: 100% Jet-A		FR_d: 25%/75% H_2/Jet-A		FR_d: 50%/50% H_2/Jet-A		FR_d: 75%/25% H_2/Jet-A		FR_d: 100% H_2	
		FR_{od}: 100% Jet-A	FR_{od}: 100% H_2	FR_{od}: 100% Jet-A	FR_{od}: 100% H_2	FR_{od}: 100% Jet-A	FR_{od}: 100% H_2	FR_{od}: 100% Jet-A	FR_{od}: 100% H_2	FR_{od}: 100% Jet-A	FR_{od}: 100% H_2
LTO take-off	T_3 (K)	953.8	953.1	954.0	953.0	954.2	953.1	954.3	953.1	954.4	953.1
	P_3 (bar)	60.0	59.9	60.0	59.9	60.1	60.0	60.1	60.0	60.1	60.0
	T_4 (K)	1796.8	1735.0	1822.9	1757.4	1837.7	1769.7	1846.7	1777.3	1853.0	1782.5
	FAR	0.0254	0.0091	0.0267	0.0094	0.0272	0.0096	0.0275	0.0097	0.0278	0.0098
	$EINO_x$_pz	40.0	82.2	45.4	102.6	47.4	113.4	48.3	119.3	48.8	123.9
	$EICO_2$	3093.5	70.9	3090.3	68.7	3088.5	67.6	3087.5	66.9	3086.7	66.4
LTO climb-out	T_3 (K)	920.0	919.0	920.1	918.9	920.2	919.0	920.3	919.0	920.4	919.0
	P_3 (bar)	51.3	51.3	51.2	51.2	51.2	51.2	51.2	51.2	51.2	51.2
	T_4 (K)	1724.5	1667.1	1750.2	1689.3	1764.2	1701.7	1773.2	1709.5	1779.5	1715.0
	FAR	0.0243	0.0086	0.0252	0.0089	0.0256	0.0090	0.0259	0.0091	0.0262	0.0092
	$EINO_x$_pz	19.6	32.5	26.1	45.2	29.8	53.7	32.2	59.1	33.8	63.0
	$EICO_2$	3099.0	75.2	3095.9	72.8	3094.2	71.5	3093.2	70.8	3092.4	70.3
LTO approach	T_3 (K)	717.6	717.6	716.3	716.4	715.7	715.8	715.3	715.3	714.9	715.0
	P_3 (bar)	19.4	19.4	19.3	19.3	19.2	19.2	19.2	19.2	19.1	19.1
	T_4 (K)	1465.3	1423.5	1484.0	1440.5	1494.1	1449.8	1500.5	1455.6	1505.1	1459.7
	FAR	0.0214	0.0076	0.0220	0.0078	0.0223	0.0079	0.0225	0.0080	0.0227	0.0080
	$EINO_x$_pz	10.0	14.0	13.0	19.2	14.8	22.5	15.8	24.9	16.6	26.5
	$EICO_2$	3110.1	84.8	3107.7	82.5	3106.5	81.3	3105.7	80.5	3105.1	80.0
LTO idle	T_3 (K)	552.5	552.1	550.6	550.3	549.7	549.3	549.0	548.7	548.6	548.3
	P_3 (bar)	6.8	6.8	6.7	6.7	6.7	6.7	6.6	6.6	6.6	6.6
	T_4 (K)	1145.5	1120.6	1157.0	1131.2	1163.3	1137.0	1167.5	1140.9	1170.5	1143.7
	FAR	0.0159	0.0056	0.0163	0.0058	0.0165	0.0059	0.0166	0.0059	0.0167	0.0059
	$EINO_x$_pz	3.4	4.0	4.2	5.3	4.7	6.0	5.1	6.6	5.3	7.0
	$EICO_2$	3133.8	112.3	3132.0	109.7	3130.9	108.4	3130.3	107.5	3129.8	107.0

Notes: FR_d denotes the design fuel blend ratio and FR_{od} denotes the off-design fuel blend ratio.

(2) The dry engine weight (core + fan) can be reduced by 6%–7% from adopting pure hydrogen fuel. Similarly to thermal efficiency, the achieved benefit is proportional to the energy fraction of hydrogen in the blended fuel.
(3) The results have shown that the change of the blend ratio of the fuel does not have any noticeable effect on the trends of varying the studied turbofan design parameters, SFN, JVR, OPR and PRn. Hence the benefits to be obtained are consistent throughout the explored ranges for a certain fuel blend ratio. However, the optimal OPR for a cycle that burns more hydrogen fraction is higher because of less turbine cooling air losses.
(4) For a multi-fuel turbofan, varying the fuel in thermally critical operating conditions could result in extra benefits. Switching the fuel towards more hydrogen fractions at TO condition could reduce the turbine inlet temperature by up to 70 K if 100% hydrogen is used.
(5) The CO_2 emissions index is weakly dependent on the typical turbofan operating conditions, and for multi-fuel turbofans it is generally proportional to the Jet-A fraction in the fuel and combustion efficiency dependent.
(6) With more hydrogen in the blended fuel, NO_x emissions index increased by up to 250% for hot LTO cycle operating points. However, the lower fuel rate of about 33% resulting from higher heating value of hydrogen reverses the conclusion for total NO_x emissions. This potential, however, largely depends on the design of the combustor.

With the conclusions above, one can consider a few strategies for using a multi-fuel combustion aircraft power plant and kick-starting the use of hydrogen with minor revisions to the aircraft. These strategies include lowering the turbine inlet temperature and cooling flow requirements in thermally critical operating conditions, designing lean burn combustor suitable for hydrogen combustion, and benefitting from CO_2 reduction.

CRediT authorship contribution statement

Xin ZHAO: Writing – review & editing, Writing – original draft, Visualization, Validation, Software, Methodology, Investigation, Funding acquisition, Formal analysis, Data curation, Conceptualization. **Tomas GRÖNSTEDT:** Writing – review & editing, Software, Resources, Formal analysis, Conceptualization. **Moritz G. KOLB:** Writing – review & editing, Project administration, Formal analysis.

Declaration of competing interest

The authors declare that they have no known competing financial interests or personal relationships that could have appeared to influence the work reported in this paper.

Acknowledgements

This work had received funding from the Horizon Europe Research and Innovation Programme (No. 101096275). This work was co-funded by UK Research and Innovation (UKRI) under the UK Government's Horizon Europe Guarantee Funding (No. 10068673).

References

1. Blakey S, Rauch B, Oldani A, et al. Advanced fuel property data platform: Overview and potential applications. *Front Energy Res* 2022;**10**:771325.
2. IATA. Energy and new fuels infrastructure net zero roadmap. Montreal: IATA; 2023.
3. Airbus. Sustainable aviation fuels – a new generation of reduced emissions fuels [Internet]. 2024 Dec 20. Available from: https://www.airbus.com/en/innovation/energy-transition/sustainable-aviation-fuels.
4. IATA. Aircraft technology net zero roadmap. Montreal: IATA; 2023.
5. ICAO. Report on the feasibility of a Long-Term Aspirational Goal (LTAG) for international civil aviation CO_2 emission reductions. Montreal: ICAO; 2022.
6. Nnabuife SG, Oko E, Kuang BY, et al. The prospects of hydrogen in achieving net zero emissions by 2050: A critical review. *Sustain Chem Clim Action* 2023;**2**:100024.
7. de Vasconcelos Leitão AB, Bringhenti C, Tomita JT, et al. A review of hydrogen aircraft propulsion systems: Recent advances and environmental perspectives. *Int J Hydrog Energy* 2025;**176**:151489.
8. Ueckerdt F, Bauer C, Dirnaichner A, et al. Potential and risks of hydrogen-based e-fuels in climate change mitigation. *Nat Clim Change* 2021;**11**(5):384–93.
9. Noble D, Wu D, Emerson B, et al. Assessment of current capabilities and near-term availability of hydrogen-fired gas turbines considering a low-carbon future. *J Eng Gas Turbines Power* 2021;**143**(4):041002.
10. Sun YZ, Cai T, Shahsavari M, et al. RANS simulations on combustion and emission characteristics of a premixed NH_3/H_2 swirling flame with reduced chemical kinetic model. *Chin J Aeronaut* 2021;**34**(12):17–27.
11. Liu CY, Gao CH, Huang Y, et al. Experimental and numerical study of combustion characteristics of ammonia–hydrogen–air swirling flame with/without secondary air injection. *Chin J Aeronaut* 2024;**37**(4):243–55.
12. Carusotto S, Goel P, Baratta M, et al. Combustion characterization in a diffusive gas turbine burner for hydrogen-compliant applications. *Energies* 2022;**15**(11):4117.
13. Park S. Hydrogen addition effect on NO formation in methane/air lean-premixed flames at elevated pressure. *Int J Hydrog Energy* 2021;**46**(50):25712–25.
14. Wang KF, Li F, Zhou T, et al. Numerical study of combustion and emission characteristics for hydrogen mixed fuel in the methane-fueled gas turbine combustor. *Aerospace* 2023;**10**(1):72.
15. Xing C, Chen XY, Qiu PH, et al. Effect of fuel flexibility on combustion performance of a micro-mixing gas turbine combustor at different fuel temperatures. *J Energy Inst* 2022;**102**:100–17.
16. Funke HH, Beckmann N, Keinz J, et al. 30 years of dry-low-NO_x micromix combustor research for hydrogen-rich fuels—An overview of past and present activities. *J Eng Gas Turbines Power* 2021;**143**(7):071002.
17. Lam KK, Geipel P, Larfeldt J. Hydrogen enriched combustion testing of siemens industrial SGT-400 at atmospheric conditions. *J Eng Gas Turbines Power* 2015;**137**(2):021502.
18. Banihabib R, Lingstädt T, Wersland M, et al. Development and testing of a 100 kW fuel-flexible micro gas turbine running on 100% hydrogen. *Int J Hydrog Energy* 2024;**49**:92–111.
19. Adler EJ, Martins JRRA. Hydrogen-powered aircraft: fundamental concepts, key technologies, and environmental impacts. *Prog Aerosp Sci* 2023;**141**:100922.

20. Bermperis D, Vouros S, Kyprianidis K. Integrated design of hydrogen-fired turboprop and commuter aircraft. *J Glob Power Propuls Soc* 2025;**9**:117–30.
21. Hoelzen J, Silberhorn D, Zill T, et al. Hydrogen-powered aviation and its reliance on green hydrogen infrastructure–review and research gaps. *Int J Hydrog Energy* 2022;**47**(5):3108–30.
22. Prewitz M, Schwärzer J, Bardenhagen A. Potential analysis of hydrogen storage systems in aircraft design. *Int J Hydrog Energy* 2023;**48**(65):25538–48.
23. Rao AG, Yin FJ, Werij HGC, et al. Energy transition in aviation: the role of cryogenic fuels. *Aerospace* 2020;**7**(12):181.
24. Sethi V, Sun XX, Nalianda D, et al. Enabling cryogenic hydrogen-based CO_2-free air transport: Meeting the demands of zero carbon aviation. *IEEE Electrific Mag* 2022;**10**(2):69–81.
25. Xisto C, Lundbladh A. Design and performance of liquid hydrogen fuelled aircraft for year 2050 EIS. *33rd congress of the international council of the aeronautical sciences*. 2022.
26. Yusaf T, Faisal Mahamude AS, Kadirgama K, et al. Sustainable hydrogen energy in aviation–A narrative review. *Int J Hydrog Energy* 2024;**52**:1026–45.
27. Yin FJ, Rao AG. Off-design performance of an interstage turbine burner turbofan engine. *J Eng Gas Turbines Power* 2017;**139**(8):082603.
28. Yin FJ, Gangoli Rao A, Bhat A, et al. Performance assessment of a multi-fuel hybrid engine for future aircraft. *Aerosp Sci Technol* 2018;**77**:217–27.
29. Yin FJ, Rao AG. A review of gas turbine engine with inter-stage turbine burner. *Prog Aerosp Sci* 2020;**121**:100695.
30. Bexten T, Jörg S, Petersen N, et al. Model-based thermodynamic analysis of a hydrogen-fired gas turbine with external exhaust gas recirculation. *J Eng Gas Turbines Power* 2021;**143**(8):081016.
31. Kahraman N, Tangöz S, Akansu SO. Numerical analysis of a gas turbine combustor fueled by hydrogen in comparison with jet-A fuel. *Fuel* 2018;**217**:66–77.
32. Grönstedt T. Development of methods for analysis and optimization of complex jet engine systems [dissertation]. Gothenburg: Chalmers University of Technology; 2000.
33. Grönstedt T, Irannezhad M, Lei X, et al. First and second law analysis of future aircraft engines. *J Eng Gas Turbines Power* 2014;**136**(3):031202.
34. Xisto C, Ali F, Petit O, et al. Analytical model for the performance estimation of pre-cooled pulse detonation turbofan engines. New York: ASME; 2017. Report No.: GT2017-63776.
35. Zhao X, Thulin O, Grönstedt T. First and second law analysis of intercooled turbofan engine. *J Eng Gas Turbines Power* 2016;**138**(2):021202.
36. Thulin O, Petit O, Xisto C, et al. First and second law analysis of radical intercooling concepts. *J Eng Gas Turbines Power* 2018;**140**(8):081201.
37. Grönstedt T, Au D, Kyprianidis K, et al. Low-pressure system component advancements and its influence on future turbofan engine emissions. New York: ASME; 2009. Report No.: GT2009-60201.
38. Korsia JJ, De Spiegeleer G. VITAL - European R&D programme for greener aero-engines. *Congress of the international council of the aeronautical sciences*. 2006.
39. Wilfert G, Sieber J, Rolt A, et al. New environmental friendly aero engine core concepts. *International symposium on air breathing engines*. 2007.
40. Larsson L, Grönstedt T, Kyprianidis KG. Conceptual design and mission analysis for a geared turbofan and an open rotor configuration. New York: ASME; 2011. Report No.: GT2011-46451.
41. Kyprianidis KG, Rolt AM, Grönstedt T. Multidisciplinary analysis of a geared fan intercooled core aero-engine. *J Eng Gas Turbines Power* 2014;**136**:011203.
42. Gordon S, McBride BJ. Computer program for calculation of complex chemical equilibrium compositions and applications. Part 1: Analysis. Washington, D.C.: NASA; 1994. Report No.: NASA-RP-1311.
43. Goodwin DG, Moffat HK, Speth RL. Cantera: An object-oriented software toolkit for chemical kinetics, thermodynamics, and transport processes. Genève: Zenodo; 2018.
44. Saggese C, Wan K, Xu R, et al. A physics-based approach to modeling real-fuel combustion chemistry–V. NO_x formation from a typical Jet A. *Combust Flame* 2020;**212**:270–8.
45. Wang H, Xu R, Wang K, et al. A physics-based approach to modeling real-fuel combustion chemistry - I. Evidence from experiments, and thermodynamic, chemical kinetic and statistical considerations. *Combust Flame* 2018;**193**:502–19.
46. Xu R, Wang K, Banerjee S, et al. A physics-based approach to modeling real-fuel combustion chemistry–II. Reaction kinetic models of jet and rocket fuels. *Combust Flame* 2018;**193**:520–37.
47. Saravanamuttoo HI, Rogers GFC, Cohen H, et al. *Gas turbine theory*. 6th ed. London: Pearson Education; 2008.
48. Chapman JW, Lavelle TM, Litt JS. Practical techniques for modeling gas turbine engine performance. *52nd AIAA/SAE/ASEE joint propulsion conference*. Reston: AIAA; 2016.
49. Görtz A, Silberhorn D. Thermodynamic potential of turbofan engines with direct combustion of hydrogen. *33rd congress of the international council of the aeronautical sciences*. 2022.
50. Woolley HW. Ideal gas thermodynamic functions for water. *J Res Natl Bur Stand* 1987;**92**(1):35.
51. Mo D, Lin YZ, Liu YX, et al. Investigation of the flow characteristics and NO_x formation mechanism of hydrogen micromix diffusion combustion with vortex generator. *Phys Fluids* 2024;**36**(12):125103.
52. Mo D, Lin YZ, Liu YX, et al. Characterization and validation of low emission mechanisms in hydrogen micromix diffusion combustor. *Appl Therm Eng* 2025;**274**:126497.
53. Singh G, Schreiner BDJ, Sun XX, et al. A review of hydrogen micromix combustion technologies for gas turbine applications. *Int J Hydrog Energy* 2025;**127**:295–310.
54. Heywood JB, Mikus T. Parameters controlling nitric oxide emissions from gas turbine combustors. Washington, D.C.: NASA; 1973. Report No.: NASA-CR-132959.
55. Naha S, Briones AM, Aggarwal SK. Effect of fuel blends on pollutant emissions in flames. *Combust Sci Technol* 2004;**177**(1):183–220.
56. Hui X, Zhang C, Xia M, et al. Effects of hydrogen addition on combustion characteristics of n-decane/air mixtures. *Combust Flame* 2014;**161**(9):2252–62.
57. Clemen C, Ravikanti M, La Bianca N, et al. Considerations for hydrogen fueled aerospace gas turbine combustion sub-system design. New York: ASME; 2024. Report No.: GT2024-122593.
58. Stebar RF, Parks FB. Emission control with lean operation using hydrogen-supplemented fuel. *SAE Trans* 1974;**83**:821–36.
59. Hiroyasu H, Arai M, Kadota T, et al. An experimental study on kerosene-hydrogen hybrid combustion in a gas turbine combustor. *Bull JSME* 1980;**23**(184):1655–62.
60. Alabaş HA, Albayrak Çeper B. Effect of the hydrogen/kerosene blend on the combustion characteristics and pollutant emissions in a mini jet engine under CDC conditions. *Int J Hydrog Energy* 2024;**52**:1275–87.
61. Saleem A, Karimi IA, Farooq S. Estimating NO_x emissions of useful two-fuel blends from literature data. *Fuel* 2022;**316**:123213.
62. Chmielewski M, Gieras M. Impact of variable geometry combustor on performance and emissions from miniature gas turbine engine. *J Energy Inst* 2017;**90**(2):257–64.

63. Chmielewski M, Niszczota P, Gieras M. Combustion efficiency of fuel-water emulsion in a small gas turbine. *Energy* 2020;**211**:118961.
64. Türkyilmaz B, Lüdemann M, Kolb MG, et al. Design of a short-to-medium-range baseline aircraft with an entry into service in 2035 for the HOPE project. *Aerospace* 2025;**12**(7):585.
65. Samuelsson S, Kyprianidis KG, Grönstedt T. Consistent conceptual design and performance modeling of aero engines. New York: ASME; 2015. Report No.: GT2015-43331.
66. Grieb H. *Projektierung von turboflugtriebwerken*. Berlin: Springer-Verlag; 2013 [German].
67. Kyprianidis KG, Rolt AM. On the optimization of a geared fan intercooled core engine design. *J Eng Gas Turbines Power* 2015;**137**(4):041201.
68. Zhao X, Sahoo S, Kyprianidis K, et al. Off-design performance analysis of hybridised aircraft gas turbine. *Aeronaut J* 2019;**123** (1270):1999–2018.
69. Sielemann M, Coïc C, Zhao X, et al. Multi-point design of parallel hybrid aero engines. *2020 AIAA/IEEE electric aircraft technologies symposium (EATS)*. Piscataway: IEEE Press; 2020.
70. Wilcock RC, Young JB, Horlock JH. The effect of turbine blade cooling on the cycle efficiency of gas turbine power cycles. *J Eng Gas Turbines Power* 2005;**127**(1):109–20.
71. Young JB, Wilcock RC. Modeling the air-cooled gas turbine: Part 2—coolant flows and losses. *J Turbomach* 2002;**124** (2):214–21.
72. Jeong Y, Vo DT, Ryu J. Effect of hydrogen combustion on film cooling characteristics in gas turbines. New York: ASME; 2025. Report No.: GT2025-153185.
73. Aygun H. Effects of air to fuel ratio on parameters of combustor used for gas turbine engines: Applications of turbojet, turbofan, turboprop and turboshaft. *Energy* 2024;**305**:132346.
74. Rolt A, Sethi V, Jacob F, et al. Scale effects on conventional and intercooled turbofan engine performance. *Aeronaut J* 2017;**121** (1242):1162–85.
75. Chandrasekaran N, Guha A. Study of prediction methods for NOx emission from turbofan engines. *J Propul Power* 2012;**28** (1):170–80.
76. Corchero G, Montañés JL. An approach to the use of hydrogen for commercial aircraft engines. *Proc Inst Mech Eng Part G J Aerosp Eng* 2005;**219**(1):35–44.
77. Jackson AJ. Optimisation of aero and industrial gas turbine design for the environment [dissertation]. Cranfield: Cranfield University; 2009.
78. ICAO. Data from: ICAO aircraft engine emissions databank. Montreal: ICAO; 2025.
79. Mourouzidis C, Singh G, Sun X, et al. Abating CO_2 and non-CO_2 emissions with hydrogen propulsion. *Aeronaut J* 2024;**128** (1325):1576–93.
80. Stürken J, Meinberg L, Bahm S, et al. Concept for a hydrogen-powered aircraft for 150 passengers with EIS 2035. *Deutscher Luft- und Raumfahrtkongress 2021*. 2021.
81. Onorato G, Proesmans P, Hoogreef MFM. Assessment of hydrogen transport aircraft: Effects of fuel tank integration. *CEAS Aeronaut J* 2022;**13**(4):813–45.
82. Silberhorn D, Atanasov G, Walther JN, et al. Assessment of hydrogen fuel tank integration at aircraft level. *Deutscher Luft- und Raumfahrtkongress 2019*. 2019.
83. Troeltsch FM, Engelmann M, Scholz AE, et al. Hydrogen powered long haul aircraft with minimized climate impact. *2020 AIAA aviation forum*. Reston: AIAA; 2020.
84. Marek C, Smith T, Kundu K. Low emission hydrogen combustors for gas turbines using lean direct injection. *41st AIAA/ASME/SAE/ASEE joint propulsion conference & exhibit*. Reston: AIAA; 2005.
85. Dave K, Link S, De Domenico F, et al. Kerosene-H_2 blending effects on flame properties in a multi-fuel combustor. *Fuel Commun* 2025;**23**:100139.
86. Ferrante G, Doodeman L, Rao AG, et al. LES of hydrogen-enriched methane flames in a lean-burn combustor with axial air injection. New York: ASME; 2023. Report No.: GT2023-103006.
87. Hatem FA, Alsaegh AS, Al-Faham M, et al. Enhancing flame flashback resistance against combustion induced vortex breakdown and boundary layer flashback in swirl burners. *Appl Energy* 2018;**230**:946–59.
88. Reichel TG, Terhaar S, Paschereit O. Increasing flashback resistance in lean premixed swirl-stabilized hydrogen combustion by axial air injection. *J Eng Gas Turbines Power* 2015;**137** (7):071503.
89. Palanti L, Mazzei L, Bianchini C, et al. CFD-based scouting for the design of a multi-fuel kerosene/hydrogen atmospheric burner. *34th congress of the international council of the aeronautical sciences*. 2024.
90. Moldanova J, Hallquist Å, Priestley M, et al. Characterisation of emissions from sustainable aviation fuels and Jet A1 fuel on turbojet engine. Stockholm: IVL Svenska Miljöinstitutet; 2024.